Review

Arzanol: A Review of Chemical Properties and Biological Activities

Yulian Voynikov *

Posted Date: 21 August 2025

doi: 10.20944/preprints202508.1508.v1

Keywords: arzanol; *Helichrysum italicum*; *Helichrysum stoechas*; anti-inflammatory; antioxidant; multitarget natural product

 doi:10.20944/preprints202508.1508.v1

Review

Arzanol: A Review of Chemical Properties and Biological Activities

Yulian Voynikov

Department of Chemistry, Faculty of Pharmacy, Medical University, 1000 Sofia, Bulgaria;
y_voynikov@pharmfac.mu-sofia.bg

Abstract

Arzanol, a prenylated phloroglucinol–α-pyrone heterodimer from *Helichrysum italicum*, displays a broad range of pharmacological properties. This review compiles scientific data from the first characterization of the compound in 2007 to present, on its chemistry, conformational behavior, bioactivities, molecular targets, and pharmacokinetics. The conformational flexibility of arzanol, driven by intramolecular hydrogen bonding, enables multitarget interactions. Arzanol shows potent anti-inflammatory activity through NF-κB inhibition and dual suppression of mPGES-1 and 5-LOX, robust antioxidant and cytoprotective effects via radical scavenging and metal chelation, and selective antibacterial activity against drug-resistant *Staphylococcus aureus*. It also modulates autophagy, mitochondrial function, and metabolic pathways, with high-affinity binding to brain glycogen phosphorylase and SIRT1. Pharmacokinetic data indicate gastrointestinal stability, intestinal absorption, and limited blood–brain barrier penetration. In vivo, arzanol exhibits neuroprotective, neurobehavioral, and metabolic effects, while showing selective cytotoxicity toward cancer cells with minimal impact on normal cells. Its multitarget profile, favorable safety, and oral bioavailability support further development for inflammatory, metabolic, and degenerative disorders.

Keywords: arzanol; *Helichrysum italicum*; *Helichrysum stoechas;* anti-inflammatory; antioxidant; multitarget natural product

1. Introduction

Arzanol, a prenylated phloroglucinol α-pyrone heterodimer, has emerged as a multifunctional bioactive natural product with diverse pharmacological properties. First isolated from Helichrysum italicum in 2007 [1], this compound has attracted significant scientific interest due to its broad spectrum of biological activities, including anti-inflammatory [1,2], antioxidant [3,4], antibacterial [5–7], cytotoxic [4,8], neuroprotective [9], antiparasitic [8] activities and many more [10–12]. This comprehensive review systematically examines the chemical characteristics, conformational behavior, biological activities, molecular targets, and pharmacokinetic properties of arzanol based on extensive studies conducted from the initial characterization of the compound in 2007 [1] to present, as summarized in Figure 2. A detailed tabulated format of biological activity assays are presented in Table 1.

2. Isolation, Natural Sources and Synthesis

Arzanol has been successfully isolated from two Mediterranean *Helichrysum* species: *H. italicum* (Roth) G. Don subsp. *microphyllum* [1,3,5,6] and *H. stoechas* (L.) Moench [13]. The compound is predominantly found in the aerial parts and inflorescences of these plants, with yields varying significantly depending on the source material and extraction methodology. Initial isolation by Appendino et al. (2007) from *H. italicum* subsp. *microphyllum* collected near Arzana (Sardinia, Italy) 0.097% w/w using acetone maceration. Subsequent studies have reported variable yields from the

 doi:10.20944/preprints202508.1508.v1

same subspecies: Rosa et al. (2007) obtained 0.081% w/w [3], while Taglialatela-Scafati et al. (2013) achieved a notably higher yield of 0.296% w/w [5]. Werner et al. (2019) reported a considerably lower yield of only 0.002% w/w [6]. *H. stoechas* has shown the highest arzanol content, with Les et al. (2017) isolating 0.48% w/w. The extraction typically involved maceration with acetone or methanol at room temperature (or 4°C for H. stoechas), followed by various chromatographic techniques including silica gel column chromatography, Sephadex LH-20, and semi-preparative HPLC.

While arzanol is naturally occurring, its total synthesis has been achieved to support structure-activity relationship studies and ensure a reliable supply for biological investigations. Minassi et al. (2012) [14] reported the first total synthesis of arzanol through a biomimetic approach that couples phloracetophenone with 6-ethyl-4-hydroxy-5-methyl-α-pyrone via a methylene bridge. Two synthetic strategies were developed, differing in the methylene source: the first employed paraformaldehyde as the methylene donor (61% yield), while the second utilized Eschenmoser's salt (65% yield). The relatively straightforward synthesis, accomplished in moderate to good yields, makes arzanol and its derivatives accessible for extensive pharmacological evaluation without relying only on natural plant resources.

3. Chemical Structure and Properties

Arzanol is a 3-prenylated acetophloroglucinol moiety linked to an α-pyrone unit through a methylene bridge. Despite its water insolubility, arzanol exhibits high solubility in polar organic solvents including methanol, ethanol, dimethyl sulfoxide (DMSO), and acetone [14].

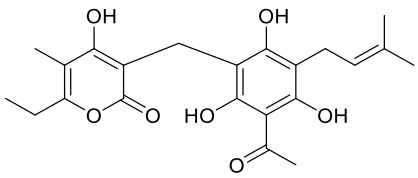

Arzanol

Chemical Formula: $C_{22}H_{26}O_7$

Exact Mass: 402.16785

3.1. Conformational Dynamics and Solution Structure

The solution structure of arzanol has been extensively investigated through a combination of experimental NMR spectroscopy and computational density functional theory (DFT) calculations [15]. These studies revealed that arzanol possesses a dynamic structure resulting from multiple conformational processes. The phenolic hydroxyl groups adjacent to the methylene bridge in the phloroglucinol (PG) moiety form intramolecular hydrogen bonding with either the carbonyl or enolic hydroxyl group of the pyrone moiety, functioning alternately as hydrogen bond donors or acceptors.

While arzanol theoretically has the potential to exist in either 2-pyrone or 4-pyrone configurations, detailed spectroscopic analysis confirmed that the 2-pyrone configuration represents the predominant roto-tautomeric state in solution [15]. This preference for the 2-pyrone form has important implications for the compound's biological activity and molecular recognition.

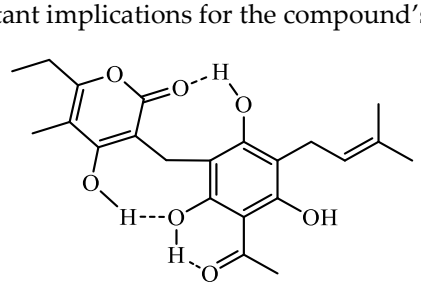

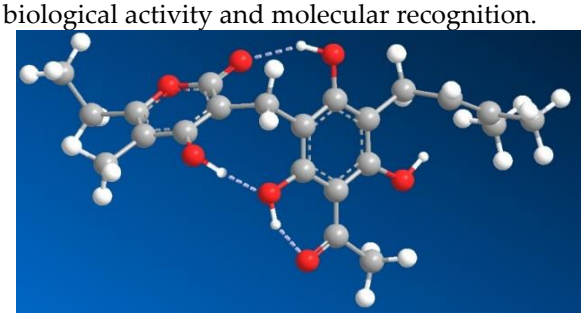

Figure 1. Intramolecular hydrogen bonding in arzanol, according to the study of Rastrelli et al. (2016) [15].

The extensive hydrogen bond network within arzanol results in a notable reduction in overall polarity, a phenomenon analogous to that observed when comparing cyclic peptides to their linear

 doi:10.20944/preprints202508.1508.v1

counterparts [15]. This intramolecular hydrogen bonding effectively shields polar groups from the surrounding solvent, potentially influencing the compound's membrane permeability and interaction with biological targets.

The conformational behavior of arzanol contrasts with that of the structurally related compound helipyrone, which exists in solution as essentially a single, monorotameric form. The presence of multiple geometric configurations enables these molecules to accommodate to various binding sites on different macromolecular targets [15]. This conformational adaptability of arzanol is hypothesized to correlate to the diverse multitarget activities.

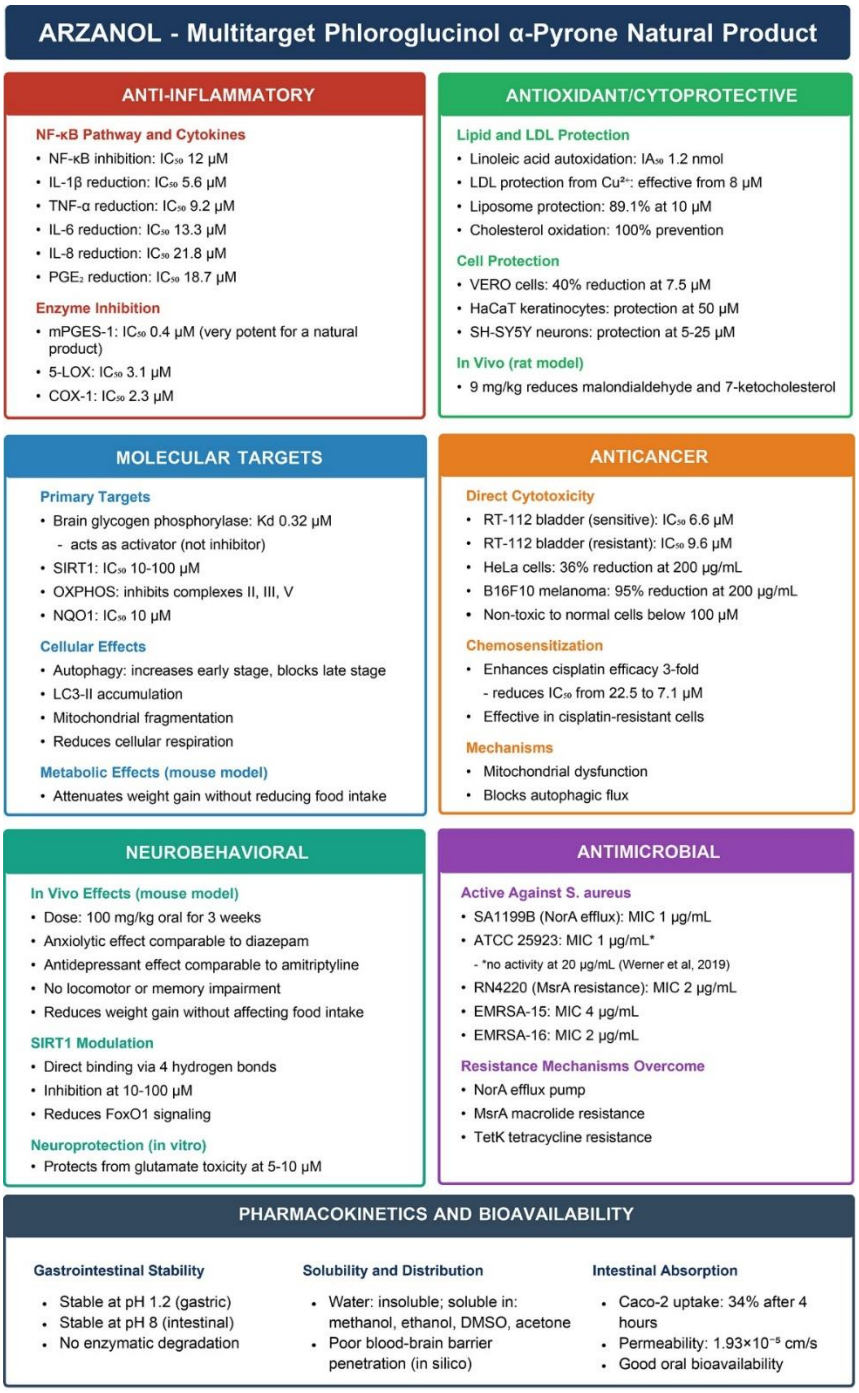

Figure 2. Summary of biological activities of arzanol.

4. Anti-inflammatory Activity

4.1. NF-κB Pathway Inhibition

 doi:10.20944/preprints202508.1508.v1

Arzanol exhibits potent anti-inflammatory activity through multiple molecular targets and signaling pathways. Arzanol inhibits nuclear factor-κB (NF-κB) signaling pathway, with an IC_{50} of approximately 12 μM [1]. This inhibition of NF-κB, a master regulator of inflammatory responses, translates to broad suppression of downstream inflammatory mediators.

Detailed dose-response studies demonstrated that arzanol effectively inhibits the production of key pro-inflammatory cytokines including interleukin-1β (IL-1β), tumor necrosis factor-α (TNF-α), interleukin-6 (IL-6), and interleukin-8 (IL-8). Additionally, the compound suppresses the production of prostaglandin E_2 (PGE_2), a critical lipid mediator of inflammation. The IC_{50} values for these various inflammatory mediators range from 5.6 to 21.8 μM, indicating consistent and potent anti-inflammatory activity across multiple targets [1].

4.2. Dual Enzymatic Inhibition

At the molecular level, arzanol functions as a dual inhibitor of two key enzymes in the arachidonic acid cascade: microsomal prostaglandin E_2 synthase-1 (mPGES-1) and 5-lipoxygenase (5-LOX). The compound inhibits mPGES-1 with remarkable potency (IC_{50} = 0.4 μM), making it one of the most potent natural mPGES-1 inhibitors identified to date. Similarly, arzanol inhibits 5-LOX with an IC_{50} of 3.1 μM, effectively blocking the production of pro-inflammatory leukotrienes [2,14].

4.3. In Vivo Validation

The anti-inflammatory efficacy of arzanol has been validated in vivo using a rat pleurisy model, a well-established model of acute inflammation. Administration of arzanol at 3.6 mg/kg significantly reduced inflammatory cell infiltration into the pleural cavity and decreased the levels of both PGE_2 and leukotrienes in the inflammatory exudate. These in vivo findings confirm that the dual inhibition of mPGES-1 and 5-LOX observed in vitro translates to meaningful anti-inflammatory effects in living organisms [2].

5. Antioxidant Activity

5.1. Protection Against Lipid Peroxidation in Lipoproteins

The antioxidant properties of arzanol have been extensively characterized across multiple biological systems. Rosa et al. (2011) conducted comprehensive studies investigating the protective effects of arzanol against lipid peroxidation in biologically relevant systems [16]. In isolated human low-density lipoproteins (LDL), a critical target in atherosclerosis development, pretreatment with arzanol provided protection against copper-induced oxidative damage.

The protection was dose-dependent, with significant effects observed starting at 8 μM concentration. Arzanol effectively preserved the levels of polyunsaturated fatty acids (PUFAs) and cholesterol while simultaneously inhibiting the formation of oxidative products including hydroperoxides and oxysterols [16]. The oxidative degradation of unsaturated fatty acids and cholesterol in biological membranes and LDL contributes significantly to tissue damage and pathological processes, particularly in cardiovascular diseases and atherosclerosis. The experimental model using copper-induced LDL oxidation at physiological temperature (37°C) closely mimics in vivo conditions, as atherosclerotic arterial walls contain trace copper ions capable of promoting LDL oxidation.

Comparative studies revealed that arzanol's protective efficacy matched that of established antioxidant standards including butylated hydroxytoluene (BHT), α-tocopherol, and the potent natural antioxidant curcumin. In liposome protection assays, arzanol demonstrated superior efficacy compared to other phenolic compounds including prenyl curcumin, homogentisic acid, vanillin, and vanillyl alcohol [4].

5.2. Mechanistic Insights into Antioxidant Action

 doi:10.20944/preprints202508.1508.v1

The antioxidant mechanism of arzanol involves multiple complementary pathways. The compound interacts with phospholipid polar heads, leading to accumulation at lipoprotein surfaces [16]. This allows arzanol to function as an effective first-line defense against oxidative attack. Direct radical scavenging occurs through hydrogen donation from the phenolic hydroxyl groups at the particle interface. Additionally, the multiple oxygenated functional groups in arzanol provide potential metal chelation sites. Computational DFT studies have elucidated the metal chelation mechanisms, identifying that the most stable arzanol-Cu^{2+} complex forms when the Cu^{2+} ion binds concurrently to the oxygen of the phenolic hydroxyl group neighboring the prenyl chain and to the π-bond of the prenyl chain itself [17]. A second highly favorable binding mode involves simultaneous coordination between the carbonyl oxygen of the α-pyrone ring and the oxygen of a nearby phenolic hydroxyl group.

5.3. Cellular Cytoprotection Against Oxidative Stress

The antioxidant properties of arzanol extend beyond simple chemical systems to provide meaningful protection in cellular models. In VERO cells (monkey kidney fibroblasts), arzanol at 7.5 μM reduced tert-butyl hydroperoxide (TBH)-induced lipid peroxidation by 40%, with no cytotoxicity observed up to 40 μM [3]. At non-cytotoxic concentrations, arzanol exerted noteworthy protection against oxidative damage in both VERO cells and differentiated Caco-2 cells (human intestinal epithelial cells), significantly decreasing the formation of oxidative products [16].

5.3.1. Protection of Skin Cells

Recent investigations have expanded understanding of arzanol's cytoprotective effects to dermatologically relevant models. Piras et al. (2024) investigated the protective effects against H_2O_2-induced oxidative stress in HaCaT human keratinocytes, a key model for skin cells [12]. Pre-incubation with arzanol (5-100 μM for 24 hours) caused no cytotoxicity or morphological alterations. When keratinocytes were subsequently challenged with cytotoxic concentrations of H_2O_2 (2.5 and 5 mM), arzanol pretreatment provided significant protection against cell death. This protective effect was linked to arzanol's ability to decrease intracellular reactive oxygen species (ROS) generation and inhibit lipid peroxidation under oxidative stress conditions. Arzanol pretreatment protected against H_2O_2-induced apoptosis, reducing the apoptotic cell population. This anti-apoptotic effect was directly associated with preservation of mitochondrial health, as arzanol prevented H_2O_2-induced mitochondrial membrane depolarization, maintaining membrane potential similar to healthy, unstressed cells [12].

5.3.2. Neuroprotection Against Oxidative Stress

The cytoprotective effects of arzanol have also been demonstrated in neuronal models. Piras et al. (2024a) investigated protection in human neuroblastoma SH-SY5Y cells subjected to H_2O_2-induced oxidative stress [18]. In differentiated SH-SY5Y cells, which more closely resemble mature neurons, pretreatment with arzanol (5-25 μM) preserved both viability and morphology when exposed to cytotoxic H_2O_2 concentrations (0.25-0.5 mM), as assessed by MTT assay. While arzanol also conferred protection in undifferentiated SH-SY5Y cells, the efficacy was less pronounced. The compound further exerted anti-apoptotic effects, lowering the baseline apoptotic/necrotic cell fraction in untreated cultures and reducing H_2O_2-induced cell death, as measured by propidium iodide staining and caspase activation assays [18].

5.4. In Vivo Antioxidant Effects

The antioxidant efficacy of arzanol has been validated in vivo using an iron-nitrilotriacetic acid (Fe-NTA) induced lipid peroxidation model in rats. Arzanol supplementation at 9 mg/kg significantly attenuated the formation of malondialdehyde (MDA) and 7-ketocholesterol (7-keto),

 doi:10.20944/preprints202508.1508.v1

two well-established markers of oxidative damage. While the impact on hydroperoxide (HP) reduction was less marked, the overall protective effect against oxidative damage was significant [4].

6. Antimicrobial Activity

The antimicrobial properties of arzanol have been evaluated against various pathogenic microorganisms, with particular emphasis on antibacterial activity.

Taglialatela-Scafati et al. (2013) reported potent antibacterial activity against a panel of six drug-resistant *Staphylococcus aureus* strains, with remarkably low minimum inhibitory concentration (MIC) values ranging from 1-4 μg/mL [5]. However, in a separate broad-spectrum antimicrobial screening, arzanol was found to be inactive at 20 μg/mL against *S. aureus* strain ATCC 25923, as well as against *Mycobacterium tuberculosis* and other tested pathogens [6]. This discrepancy in antibacterial activity may reflect several factors including differences in assay conditions, culture media composition, or strain-specific susceptibility patterns. The variation highlights the importance of comprehensive screening against multiple strains and the potential for arzanol to exhibit selective antibacterial activity.

7. Molecular Targets and Mechanisms

7.1. Brain Glycogen Phosphorylase

A study by del Gaudio et al. (2018) utilized an MS-based proteomics to investigate the cellular interactome of arzanol and identify its direct molecular targets [10]. This study identified brain glycogen phosphorylase (bGP), a key enzyme in glucose metabolism, as the main high-affinity target of arzanol.

The identification was achieved using an experimental design employing arzanol-functionalized agarose beads to "fish" for binding partners from complex HeLa cell protein lysates. The direct physical interaction between arzanol and bGP was subsequently validated using Drug Affinity Responsive Target Stability (DARTS) assays, which demonstrated that arzanol protects bGP from proteolytic degradation in a dose-dependent manner, confirming specific binding.

Detailed characterization of the arzanol-bGP interaction revealed several important features. Competitive binding assays demonstrated that adenosine monophosphate (AMP), the natural allosteric activator of bGP, prevented arzanol from binding to the enzyme. This suggested that arzanol interacts with bGP at the same allosteric binding site as AMP. Surface Plasmon Resonance (SPR) analysis confirmed direct, high-affinity binding with a measured dissociation constant (Kd) of 0.32 ± 0.15 μM, indicating a physiologically relevant interaction [10].

These experimental findings were corroborated by computational molecular docking studies, which predicted that arzanol's most favorable binding pose occurs within the AMP allosteric pocket. Functional assays performed with HeLa cell lysates revealed that arzanol increases the catalytic activity of bGP in a concentration-dependent manner. This establishes arzanol not as an inhibitor, but as a positive modulator (activator) of bGP, representing a novel activity for this class of phloroglucinol-pyrone compounds [10].

7.2. Autophagy Modulation and Mitochondrial Dysfunction

Deitersen et al. (2021) identified arzanol as a modulator of autophagy through a high-throughput screen and subsequently characterized its anticancer effects and molecular mechanism of action in detail [11]. This study revealed that arzanol exhibits complex, dual-stage effects on the autophagy pathway.

Initially identified as an inhibitor of late-stage autophagic flux, this activity was confirmed by arzanol's ability to cause significant accumulation of lipidated LC3-II and the autophagy receptor p62/SQSTM1 in HeLa cells. However, more detailed investigation revealed that while inhibiting the final stages of autophagy, arzanol simultaneously acts as an inducer of early autophagosome

 doi:10.20944/preprints202508.1508.v1

biogenesis. This was evidenced by a significant increase in the number of ATG16L1-positive structures and the formation of numerous, albeit smaller-than-usual, autophagosomes [11].

7.2.1. Mitochondrial Toxicity as a Mechanism of Action

The underlying mechanism for arzanol's cellular effects was identified as direct mitochondrial toxicity. The study characterized arzanol as a mitotoxin—a compound that specifically induces mitochondrial damage. Multiple lines of evidence supported this characterization: arzanol caused significant mitochondrial fragmentation observable by microscopy and induced a sharp reduction in mitochondrial respiration measured by oxygen consumption [11].

Detailed biochemical analysis traced the respiratory impairment to direct inhibition of multiple oxidative phosphorylation (OXPHOS) complexes, specifically complexes II, III, and V. Additionally, arzanol inhibited NADH:quinone oxidoreductase 1 (NQO1), another mitochondria-associated oxidoreductase. This multi-target mitochondrial inhibition likely underlies the compound's cytotoxic effects [11].

7.3. Anticancer Activity and Chemosensitization

The mitochondrial dysfunction induced by arzanol translates to meaningful anticancer activity. In urothelial bladder carcinoma models, arzanol exhibited moderate cytotoxicity as a single agent, with IC_{50} values of 6.6 μM in cisplatin-sensitive and 9.6 μM in cisplatin-resistant RT-112 cells. Importantly, arzanol demonstrated significant activity as a chemosensitizer. When used in combination with the standard chemotherapeutic cisplatin, arzanol enhanced its potency approximately threefold, reducing cisplatin's IC_{50} from 22.5 μM to 7.1 μM in sensitive cancer cells [11].

7.4. SIRT1 Inhibition and Metabolic Regulation

Borgonetti et al. (2023) identified sirtuin 1 (SIRT1) as another important molecular target of arzanol [9]. Molecular docking studies revealed that arzanol binds to SIRT1 through a network of four hydrogen bonds involving residues Arg274, Tyr280, Gln345, and Ile347. This predicted binding was validated through enzyme inhibition assays, which demonstrated that arzanol exhibits SIRT1 inhibitory activity comparable to or superior to nicotinamide (a known SIRT1 inhibitor) at concentrations of 10-100 μM.

Ex vivo studies using mouse hippocampal tissue confirmed the physiological relevance of SIRT1 inhibition. Arzanol treatment reduced both SIRT1 protein expression and enzymatic activity, with concurrent downregulation of FoxO1 signaling, a key downstream target of SIRT1. This SIRT1 inhibition likely contributes to arzanol's metabolic and neurobehavioral effects [9].

8. Pharmacokinetics and Bioavailability

8.1. Gastrointestinal Stability

A critical factor in the development of orally active natural products is their stability under gastrointestinal conditions. Silva et al. (2017) investigated the gastrointestinal stability of arzanol present in aqueous decoctions of *Helichrysum stoechas* using a validated in vitro digestion model [19]. The extracts containing arzanol were subjected to sequential treatment mimicking the digestive process: first with artificial gastric juice (pepsin buffered at pH 1.2) followed by artificial pancreatic juice (pancreatin buffered at pH 8), at physiological temperature (37°C) for a total of 4 hours. HPLC analysis comparing the extracts before and after the digestion process revealed stability. Arzanol was not enzymatically degraded or chemically modified during the simulated gastric and intestinal digestion. The chromatographic profile remained unchanged, and no loss of arzanol content was detected. These results provide evidence that following oral ingestion, arzanol is likely to reach the small intestine in its intact, bioactive form [19].

 doi:10.20944/preprints202508.1508.v1

8.2. Intestinal Absorption and Cellular Transport

Rosa et al. (2011) provided insights into the bioavailability of arzanol using the Caco-2 cell monolayer model, the gold standard for predicting intestinal absorption of drug candidates [16]. The Caco-2 model mimics the human intestinal barrier, including the expression of relevant transporters and metabolic enzymes.

Time-course studies revealed that arzanol accumulates inside Caco-2 epithelial cells in a time-dependent manner. After 4 hours of incubation, approximately 34% of the applied arzanol was found within the cells, indicating significant cellular uptake. More importantly, transport studies demonstrated that arzanol was able to pass through the Caco-2 cell monolayer, providing direct evidence for its potential for oral absorption [16].

8.3. Blood-Brain Barrier Penetration

While arzanol shows promising oral bioavailability, in silico pharmacokinetic modeling performed by Piras et al. (2024) predicted poor blood-brain barrier (BBB) penetration. This limitation may restrict the compound's direct effects on the central nervous system, although peripheral actions could still influence brain function through indirect mechanisms. The poor BBB penetration contrasts with the observed neurobehavioral effects, suggesting that these may be mediated through peripheral targets or metabolites [18].

9. Neurobehavioral and Metabolic Effects

9.1. Anxiolytic and Antidepressant Properties

Borgonetti et al. (2023) conducted comprehensive in vivo studies investigating the neurobehavioral effects of a methanolic extract of *Helichrysum stoechas* inflorescences, with arzanol as the principal bioactive constituent [9]. Repeated oral administration of the extract (100 mg/kg daily for 3 weeks) in mice produced significant anxiolytic effects comparable to the benzodiazepine diazepam and antidepressant-like effects comparable to the tricyclic antidepressant amitriptyline.

Importantly, these beneficial effects were achieved without the common side effects associated with conventional anxiolytics and antidepressants. The arzanol-containing extract did not impair locomotor activity or memory function, suggesting a favorable safety profile for potential therapeutic use [9].

9.2. Metabolic Effects and Weight Management

In vivo studies demonstrated that repeated oral administration of the extract of *Helichrysum stoechas* inflorescence (100 mg/kg for 3 weeks) significantly attenuated body weight gain in mice without reducing food intake [9]. This suggests that arzanol may influence metabolic processes, potentially through its effects on SIRT1 and related metabolic pathways. The ability to prevent weight gain without affecting appetite could potentially have important implications for metabolic health and obesity management.

9.3. Direct Neuroprotective Effects

In addition to systemic neurobehavioral effects, arzanol demonstrated direct neuroprotective properties in vitro. At concentrations of 5-10 μM, arzanol protected SH-SY5Y neuroblastoma cells against glutamate-induced excitotoxicity [9]. Glutamate excitotoxicity is a major mechanism of neuronal death in various neurological conditions including stroke, traumatic brain injury, and neurodegenerative diseases. The ability of arzanol to protect against this form of neuronal damage suggests potential applications in neuroprotection.

10. Cytotoxicity Profile and Selectivity

 doi:10.20944/preprints202508.1508.v1

The cytotoxic effects of arzanol have been evaluated across multiple cancer cell lines to assess its potential as an anticancer agent and to establish its selectivity profile. Rosa et al. (2017) conducted detailed dose-response studies revealing selective cytotoxicity patterns [4].

Arzanol exhibited dose-dependent cytotoxicity against HeLa cells (human cervical carcinoma) and B16F10 cells (murine melanoma). However, the most pronounced effects were observed in Caco-2 colon cancer cells, suggesting potential selectivity for gastrointestinal cancers. Critically, no significant cytotoxicity was observed at concentrations below 100 μM in normal cell lines, indicating a favorable therapeutic window [4].

This selectivity profile is particularly important for potential therapeutic development, as it suggests that arzanol may preferentially target cancer cells while sparing normal tissues at therapeutically relevant concentrations.

11. Structure-Activity Relationships and Future Perspectives

The conformational flexibility of arzanol, arising from its dynamic hydrogen bonding network, appears to be a key factor in its multitarget biological activities. The ability to adopt multiple conformations allows arzanol to interact with diverse biological targets ranging from enzymes (bGP, SIRT1, mPGES-1, 5-LOX) to cellular structures (mitochondria) and signaling pathways (NF-κB, autophagy). Future research directions should focus on:

- SAR studies to identify key pharmacophores for each activity
- Synthesis of analogs with greater potency/selectivity
- Formulations to improve solubility and BBB penetration
- Clinical validation in inflammatory, metabolic and neurodegenerative diseases
- Investigation of potential drug-drug interactions given the multiple molecular targets
- Long-term safety evaluation for chronic use

Conclusion

Arzanol represents a remarkable example of a multitarget natural product with well-characterized biological activities spanning anti-inflammatory, antioxidant, antimicrobial, and neuroprotective effects. Its unique structural features, particularly the conformational flexibility arising from intramolecular hydrogen bonding, enable interaction with diverse molecular targets.

The compound demonstrates gastrointestinal stability and intestinal absorption. While limited blood-brain barrier penetration may restrict direct central nervous system applications, the observed neurobehavioral effects suggest that peripheral actions may influence brain function.

With its favorable safety profile, including selectivity for cancer cells and lack of cytotoxicity to normal cells at therapeutic concentrations, as well as the multi-target mechanism of action positions arzanol as a promising candidate for complex diseases. As research continues to elucidate the full therapeutic potential of arzanol, this phloroglucinol-pyrone natural product exemplifies how conformational flexibility and multitarget activity can be advantageous features in drug development.

Table 1. Summary of arzanol's biological activities, effective concentrations, and experimental models.

Category	Subcategory	Biological Activity	IC50/EC50 /Dose	Model/Cell Type	Ref.
Anti-inflammatory	NF-κB Pathway	Switches off NF-κB in Jurkat immune-cell assay	IC50 ~5 μg/mL (≈12 μM)	Jurkat cells	[1]
Anti-inflammatory	Cytokine Inhibition	IL-1β reduction	IC50 5.6 μM	LPS-stimulated human monocytes	[1]

 doi:10.20944/preprints202508.1508.v1

Anti-inflammatory	Cytokine Inhibition	TNF-α reduction	IC50 9.2 μM	LPS-stimulated human monocytes	[1]
Anti-inflammatory	Cytokine Inhibition	IL-6 reduction	IC50 13.3 μM	LPS-stimulated human monocytes	[1]
Anti-inflammatory	Cytokine Inhibition	IL-8 reduction	IC50 21.8 μM	LPS-stimulated human monocytes	[1]
Anti-inflammatory	Eicosanoid Pathway	PGE_2 reduction	IC50 18.7 μM	LPS-stimulated human monocytes	[1]
Anti-inflammatory	Eicosanoid Pathway	5-LOX inhibition	IC50 3.1 μM	Recombinant enzyme assay	[2]
Anti-inflammatory	Eicosanoid Pathway	5-LOX inhibition in neutrophils (A23187/AA stimulation)	IC50 2.9 μM	Human neutrophils	[2]
Anti-inflammatory	Eicosanoid Pathway	5-LOX inhibition in neutrophils (LPS/fMLP stimulation)	IC50 8.1 μM	Human neutrophils	[2]
Anti-inflammatory	Eicosanoid Pathway	mPGES-1 inhibition	IC50 0.4 μM	IL-1β-stimulated A549 cells	[2]
Anti-inflammatory	Eicosanoid Pathway	COX-1 inhibition (12-HHT reduction)	IC50 2.3 μM	Human platelets	[2]
Anti-inflammatory	Eicosanoid Pathway	COX-1 inhibition (TXB_2 reduction)	IC50 2.9 μM	Human platelets	[2]
Anti-inflammatory	Eicosanoid Pathway	PGE_2 reduction in whole blood	~50% at 30 μM	Human whole blood	[2]
Anti-inflammatory	In Vivo	Reduces pleural fluid volume	59% at 3.6 mg/kg	Rat pleurisy model	[2]
Anti-inflammatory	In Vivo	Reduces inflammatory cell infiltration	48% at 3.6 mg/kg	Rat pleurisy model	[2]
Anti-inflammatory	In Vivo	Reduces PGE_2 levels	47% at 3.6 mg/kg	Rat pleurisy model	[2]
Anti-inflammatory	In Vivo	Reduces LTB_4 levels	31% at 3.6 mg/kg	Rat pleurisy model	[2]
Antioxidant/Cytoprotective	Lipid Protection	Complete inhibition of linoleic acid autoxidation	IA50 1.2 nmol	Solvent-free film (37°C, 32h)	[3]
Antioxidant/Cytoprotective	Lipid Protection	Protection under EDTA-mediated oxidation	≥80% at 1 nmol, 100% at ≥2.5 nmol	Linoleic acid + EDTA	[3]
Antioxidant/Cytoprotective	Lipid Protection	Protection in $FeCl_3$-catalyzed oxidation	13% at 40 nmol, 80% at 80 nmol	Linoleic acid + $FeCl_3$	[3]

 doi:10.20944/preprints202508.1508.v1

Antioxidant/Cytoprotective	Cholesterol Protection	Complete protection against cholesterol oxidation	100% at 10 nmol	140°C thermal oxidation	[3]
Antioxidant/Cytoprotective	Cholesterol Protection	Prevention of 7-keto and 7β-OH formation	IA50 5.6-6.8 nmol	140°C, 1-2h	[4]
Antioxidant/Cytoprotective	LDL Protection	Protects LDL from Cu^{2+}-induced oxidation	Significant from 8 μM	Human LDL (37°C, 2h)	[16]
Antioxidant/Cytoprotective	Liposome Protection	Protection of polyunsaturated fatty acids	89.1% at 10 μM	Phospholipid liposomes + Cu^{2+}	[4]
Antioxidant/Cytoprotective	Cell Protection	No cytotoxicity to VERO cells	Up to 40 μM	VERO fibroblasts	[3]
Antioxidant/Cytoprotective	Cell Protection	Reduces lipid peroxidation in VERO cells	40% reduction at 7.5 μM	VERO cells + 750 μM TBH	[3]
Antioxidant/Cytoprotective	Cell Protection	No cytotoxicity to VERO cells	Up to 50 μM	VERO cells (24h)	[16]
Antioxidant/Cytoprotective	Cell Protection	No cytotoxicity to differentiated Caco-2	Up to 100 μM	Differentiated Caco-2 (24h)	[16]
Antioxidant/Cytoprotective	Cell Protection	Protects VERO cells from TBH	Significant at 25-50 μM	VERO cells + TBH	[16]
Antioxidant/Cytoprotective	Cell Protection	Protects Caco-2 cells from TBH	Significant from 25 μM	Differentiated Caco-2 + TBH	[16]
Antioxidant/Cytoprotective	In Vivo	Prevents plasma lipid consumption	9 mg/kg i.p.	Wistar rats + Fe-NTA	[4]
Antioxidant/Cytoprotective	In Vivo	Protects plasma unsaturated fatty acids	Complete at 9 mg/kg	Wistar rats + Fe-NTA	[4]
Antioxidant/Cytoprotective	In Vivo	Reduces plasma MDA levels	9 mg/kg	Wistar rats + Fe-NTA	[4]
Antioxidant/Cytoprotective	In Vivo	Reduces plasma 7-ketocholesterol	9 mg/kg	Wistar rats + Fe-NTA	[4]
Antioxidant/Cytoprotective	Keratinocyte Protection	No cytotoxicity	5-100 μM	HaCaT cells	[12]
Antioxidant/Cytoprotective	Keratinocyte Protection	Protects against H_2O_2 cytotoxicity	50 μM pre-treatment	HaCaT cells + 2.5-5 mM H_2O_2	[12]
Antioxidant/Cytoprotective	Keratinocyte Protection	Reduces ROS generation	50 μM	HaCaT cells + 0.5-5 mM H_2O_2	[12]

 doi:10.20944/preprints202508.1508.v1

Antioxidant/Cytoprotective	Keratinocyte Protection	Prevents lipid peroxidation	50 μM	HaCaT cells + 2.5-5 mM H_2O_2	[12]
Antioxidant/Cytoprotective	Keratinocyte Protection	Prevents apoptosis (caspase-3/7)	50 μM	HaCaT cells + 5 mM H_2O_2	[12]
Antioxidant/Cytoprotective	Keratinocyte Protection	Preserves mitochondrial membrane potential	50 μM	HaCaT cells + 5 mM H_2O_2	[12]
Antioxidant/Cytoprotective	Neuronal Protection	Increases viability (differentiated cells)	5-25 μM	Differentiated SH-SY5Y	[18]
Antioxidant/Cytoprotective	Neuronal Protection	Cytotoxic at high dose (differentiated cells)	71% reduction at 100 μM	Differentiated SH-SY5Y	[18]
Antioxidant/Cytoprotective	Neuronal Protection	Non-toxic (undifferentiated cells)	2.5-100 μM	Undifferentiated SH-SY5Y	[18]
Antioxidant/Cytoprotective	Neuronal Protection	Protects differentiated cells from H_2O_2	5-25 μM	Differentiated SH-SY5Y + 0.5 mM H_2O_2	[18]
Antioxidant/Cytoprotective	Neuronal Protection	Protects undifferentiated cells from H_2O_2	5 μM	Undifferentiated SH-SY5Y + 0.5 mM H_2O_2	[18]
Antioxidant/Cytoprotective	Neuronal Protection	Reduces ROS (differentiated cells)	5-25 μM	Differentiated SH-SY5Y + H_2O_2	[18]
Antioxidant/Cytoprotective	Neuronal Protection	Reduces ROS (undifferentiated cells)	5 μM	Undifferentiated SH-SY5Y + H_2O_2	[18]
Antioxidant/Cytoprotective	Neuronal Protection	Decreases basal apoptosis	5-25 μM	Differentiated SH-SY5Y	[18]
Antioxidant/Cytoprotective	Neuronal Protection	Protects from H_2O_2-induced apoptosis (PI assay)	10-25 μM	ifferentiated SH-SY5Y + 0.25 mM H_2O_2	[18]
Antioxidant/Cytoprotective	Neuronal Protection	Protects from H_2O_2-induced apoptosis (caspase)	10-25 μM	Differentiated SH-SY5Y + 0.25 mM H_2O_2	[18]
Neuroprotective/Neurobehavioral	Neuroprotection	Protects from glutamate toxicity	5-10 μM	SH-SY5Y neuroblastoma cells	[9]
Neuroprotective/Neurobehavioral	Metabolic Effects	Attenuates weight gain (no effect on food intake)	100 mg/kg, 3 weeks oral	Mice	[9]
Neuroprotective/Neurobehavioral	Behavioral Effects	Anxiolytic effect (comparable to diazepam)	100 mg/kg	Mice	[9]

 doi:10.20944/preprints202508.1508.v1

Neuroprotective/Neurobehavioral	Behavioral Effects	Antidepressant effect (comparable to amitriptyline)	100 mg/kg	Mice	[9]
Neuroprotective/Neurobehavioral	Behavioral Effects	No locomotor or memory impairment	100 mg/kg	Mice	[9]
Neuroprotective/Neurobehavioral	SIRT1 Modulation	Binds SIRT1 via 4 H-bonds	Molecular docking	In silico	[9]
Neuroprotective/Neurobehavioral	SIRT1 Modulation	SIRT1 inhibition	10-100 μM	Cell-free assay	[9]
Neuroprotective/Neurobehavioral	SIRT1 Modulation	Reduces SIRT1 expression/activity	100 mg/kg HSE or 10 μM	Mouse hippocampus (ex vivo)	[9]
Neuroprotective/Neurobehavioral	SIRT1 Modulation	Suppresses FoxO1 signaling	100 mg/kg HSE or 10 μM	Cell and tissue studies	[9]
Anticancer	Autophagy Modulation	Inhibits starvation-induced autophagy	+164.6% mCitrine-LC3	Mouse embryonic fibroblasts	[11]
Anticancer	Autophagy Modulation	Accumulates LC3-II and p62/SQSTM1	Not specified	HeLa cells	[11]
Anticancer	Autophagy Modulation	Increases but reduces size of autophagosomes	Not specified	HeLa cells	[11]
Anticancer	Autophagy Modulation	Increases ATG16L1-positive structures	Not specified	HeLa cells	[11]
Anticancer	Direct Cytotoxicity	Cytotoxic to cisplatin-sensitive bladder cancer	IC50 6.6 μM	RT-112 cells	[11]
Anticancer	Direct Cytotoxicity	Cytotoxic to cisplatin-resistant bladder cancer	IC50 9.6 μM	RT-112 cells	[11]
Anticancer	Direct Cytotoxicity	Cytotoxic to undifferentiated Caco-2	55% reduction at 100 μM	Undifferentiated Caco-2	[4]
Anticancer	Direct Cytotoxicity	Cytotoxic to HeLa cells	36% reduction at 200 μg/mL	HeLa cells (24h)	[4]
Anticancer	Direct Cytotoxicity	Cytotoxic to B16F10 cells	95% reduction at 200 μg/mL	B16F10 melanoma (24h)	[4]

 doi:10.20944/preprints202508.1508.v1

Anticancer	Direct Cytotoxicity	No cytotoxicity to differentiated Caco-2	Up to 100 μM	Differentiated Caco-2	[4]
Anticancer	Direct Cytotoxicity	No cytotoxicity to L5178Y cells	20 μg/mL	Murine lymphoma L5178Y	[6]
Anticancer	Chemosensitization	Enhances cisplatin effect	Reduces IC50 from 22.5 to 7.1 μM	RT-112 cells	[11]
Anticancer	Mitochondrial Effects	Induces mitochondrial fragmentation	Not specified	HeLa cells	[11]
Anticancer	Mitochondrial Effects	Reduces basal/maximal respiration	Not specified	HeLa cells	[11]
Anticancer	Mitochondrial Effects	Inhibits OXPHOS complexes II, III, V	Not specified	Isolated mitochondria	[11]
Anticancer	Mitochondrial Effects	Inhibits NQO1	Significant at 10 μM	Direct activity assay	[11]
Metabolic	Glycogen Metabolism	Binds brain Glycogen Phosphorylase (bGP)	Identified as main target	HeLa cell lysates	[10]
Metabolic	Glycogen Metabolism	Direct bGP binding (DARTS confirmed)	Dose-dependent protection	DARTS assay	[10]
Metabolic	Glycogen Metabolism	Binds at AMP allosteric site	Competitive with AMP	Competitive binding assay	[10]
Metabolic	Glycogen Metabolism	High-affinity bGP binding	Kd = 0.32 ± 0.15 μM	Surface Plasmon Resonance	[10]
Metabolic	Glycogen Metabolism	Predicted AMP site binding	Kd,pred = 0.65 ± 0.18 μM	Molecular docking	[10]
Metabolic	Glycogen Metabolism	Activates bGP enzyme	Dose-dependent activation	HeLa cell lysates	[10]
Antibacterial	S. aureus (drug-resistant)	SA1199B (NorA efflux) inhibition	MIC 1 μg/mL	S. aureus SA1199B	[5]
Antibacterial	S. aureus (drug-resistant)	XU212 (TetK) inhibition	MIC 4 μg/mL	S. aureus XU212	[5]
Antibacterial	S. aureus (drug-resistant)	ATCC 25923 (reference) inhibition	MIC 1 μg/mL	S. aureus ATCC 25923, Mueller-Hinton/MTT method	[5]

 doi:10.20944/preprints202508.1508.v1

Antibacterial	S. aureus (drug-resistant)	RN4220 (MsrA) inhibition	MIC 2 µg/mL	S. aureus RN4220	[5]
Antibacterial	S. aureus (drug-resistant)	EMRSA-15 (epidemic MRSA) inhibition	MIC 4 µg/mL	S. aureus EMRSA-15	[5]
Antibacterial	S. aureus (drug-resistant)	EMRSA-16 (epidemic MRSA) inhibition	MIC 2 µg/mL	S. aureus EMRSA-16	[5]
Antibacterial	Negative Results	No activity against S. aureus ATCC 25923	No inhibition at 20 µg/mL	S. aureus ATCC 25923, CLSI broth microdilution	[6]

Data Availability Statement: No new data were created or analyzed in this study.

Acknowledgments: The author acknowledge the support from by the European Union-NextGenerationEU through the National Recovery and Resilience Plan of the Republic of Bulgaria, project BG-RRP-2.004-0004-C01.

Conflicts of Interest: The authors declare no conflicts of interest.

Reference

1. Appendino, G.; Ottino, M.; Marquez, N.; Bianchi, F.; Giana, A.; Ballero, M.; Sterner, O.; Fiebich, B.L.; Munoz, E. Arzanol, an anti-inflammatory and anti-HIV-1 phloroglucinol α-pyrone from Helichrysum italicum ssp. microphyllum. *Journal of natural products* **2007**, *70*, 608-612.
2. Bauer, J.; Koeberle, A.; Dehm, F.; Pollastro, F.; Appendino, G.; Northoff, H.; Rossi, A.; Sautebin, L.; Werz, O. Arzanol, a prenylated heterodimeric phloroglucinyl pyrone, inhibits eicosanoid biosynthesis and exhibits anti-inflammatory efficacy in vivo. *Biochemical pharmacology* **2011**, *81*, 259-268.
3. Rosa, A.; Deiana, M.; Atzeri, A.; Corona, G.; Incani, A.; Melis, M.P.; Appendino, G.; Dessì, M.A. Evaluation of the antioxidant and cytotoxic activity of arzanol, a prenylated α-pyrone–phloroglucinol etherodimer from Helichrysum italicum subsp. microphyllum. *Chemico-Biological Interactions* **2007**, *165*, 117-126.
4. Rosa, A.; Atzeri, A.; Nieddu, M.; Appendino, G. New insights into the antioxidant activity and cytotoxicity of arzanol and effect of methylation on its biological properties. *Chemistry and physics of lipids* **2017**, *205*, 55-64.
5. Taglialatela-Scafati, O.; Pollastro, F.; Chianese, G.; Minassi, A.; Gibbons, S.; Arunotayanun, W.; Mabebie, B.; Ballero, M.; Appendino, G. Antimicrobial phenolics and unusual glycerides from Helichrysum italicum subsp. microphyllum. *Journal of natural products* **2013**, *76*, 346-353.
6. Werner, J.; Ebrahim, W.; Özkaya, F.C.; Mándi, A.; Kurtán, T.; El-Neketi, M.; Liu, Z.; Proksch, P. Pyrone derivatives from Helichrysum italicum. *Fitoterapia* **2019**, *133*, 80-84.
7. D'Abrosca, B.; Buommino, E.; Caputo, P.; Scognamiglio, M.; Chambery, A.; Donnarumma, G.; Fiorentino, A. Phytochemical study of Helichrysum italicum (Roth) G. Don: Spectroscopic elucidation of unusual amino-phlorogucinols and antimicrobial assessment of secondary metabolites from medium-polar extract. *Phytochemistry* **2016**, *132*, 86-94, doi:https://doi.org/10.1016/j.phytochem.2016.09.012.
8. Akaberi, M.; Danton, O.; Tayarani-Najaran, Z.; Asili, J.; Iranshahi, M.; Emami, S.A.; Hamburger, M. HPLC-Based Activity Profiling for Antiprotozoal Compounds in the Endemic Iranian Medicinal Plant Helichrysum oocephalum. *Journal of Natural Products* **2019**, *82*, 958-969, doi:10.1021/acs.jnatprod.8b01031.
9. Borgonetti, V.; Caroli, C.; Governa, P.; Virginia, B.; Pollastro, F.; Franchini, S.; Manetti, F.; Les, F.; López, V.; Pellati, F.; Galeotti, N. Helichrysum stoechas (L.) Moench reduces body weight gain and modulates mood disorders via inhibition of silent information regulator 1 (SIRT1) by arzanol. *Phytotherapy Research* **2023**, *37*, 4304-4320, doi:https://doi.org/10.1002/ptr.7941.

 doi:10.20944/preprints202508.1508.v1

10. del Gaudio, F.; Pollastro, F.; Mozzicafreddo, M.; Riccio, R.; Minassi, A.; Monti, M.C. Chemoproteomic fishing identifies arzanol as a positive modulator of brain glycogen phosphorylase. *Chemical Communications* **2018**, *54*, 12863-12866, doi:10.1039/C8CC07692H.
11. Deitersen, J.; Berning, L.; Stuhldreier, F.; Ceccacci, S.; Schlütermann, D.; Friedrich, A.; Wu, W.; Sun, Y.; Böhler, P.; Berleth, N. High-throughput screening for natural compound-based autophagy modulators reveals novel chemotherapeutic mode of action for arzanol. *Cell Death & Disease* **2021**, *12*, 560.
12. Piras, F.; Sogos, V.; Pollastro, F.; Appendino, G.; Rosa, A. Arzanol, a natural phloroglucinol α-pyrone, protects HaCaT keratinocytes against H2O2-induced oxidative stress, counteracting cytotoxicity, reactive oxygen species generation, apoptosis, and mitochondrial depolarization. *Journal of Applied Toxicology* **2024**, *44*, 720-732, doi:https://doi.org/10.1002/jat.4570.
13. Les, F.; Venditti, A.; Cásedas, G.; Frezza, C.; Guiso, M.; Sciubba, F.; Serafini, M.; Bianco, A.; Valero, M.S.; López, V. Everlasting flower (Helichrysum stoechas Moench) as a potential source of bioactive molecules with antiproliferative, antioxidant, antidiabetic and neuroprotective properties. *Industrial crops and products* **2017**, *108*, 295-302.
14. Minassi, A.; Cicione, L.; Koeberle, A.; Bauer, J.; Laufer, S.; Werz, O.; Appendino, G. A Multicomponent Carba-Betti Strategy to Alkylidene Heterodimers–Total Synthesis and Structure–Activity Relationships of Arzanol. **2012**.
15. Rastrelli, F.; Bagno, A.; Appendino, G.; Minassi, A. Bioactive Phloroglucinyl Heterodimers: The Tautomeric and Rotameric Equlibria of Arzanol. *European Journal of Organic Chemistry* **2016**, *2016*, 4810-4816, doi:https://doi.org/10.1002/ejoc.201600597.
16. Rosa, A.; Pollastro, F.; Atzeri, A.; Appendino, G.; Melis, M.P.; Deiana, M.; Incani, A.; Loru, D.; Dessì, M.A. Protective role of arzanol against lipid peroxidation in biological systems. *Chemistry and Physics of Lipids* **2011**, *164*, 24-32, doi:https://doi.org/10.1016/j.chemphyslip.2010.09.009.
17. Mammino, L. Complexes of arzanol with a Cu2+ ion: a DFT study. *Journal of Molecular Modeling* **2017**, *23*, 276, doi:10.1007/s00894-017-3443-4.
18. Piras, F.; Sogos, V.; Pollastro, F.; Rosa, A. Protective effect of arzanol against H2O2-induced oxidative stress damage in differentiated and undifferentiated SH-SY5Y Cells. *International Journal of Molecular Sciences* **2024**, *25*, 7386.
19. Silva, L.; Rodrigues, A.M.; Ciriani, M.; Falé, P.L.V.; Teixeira, V.; Madeira, P.; Machuqueiro, M.; Pacheco, R.; Florêncio, M.H.; Ascensão, L.; Serralheiro, M.L.M. Antiacetylcholinesterase activity and docking studies with chlorogenic acid, cynarin and arzanol from Helichrysum stoechas (Lamiaceae). *Medicinal Chemistry Research* **2017**, *26*, 2942-2950, doi:10.1007/s00044-017-1994-7.